

Application of Magnesium Hydroxide for the Remediation of Acid Mine Drainage

Jacobeth Galane¹, Tholiso Ngulube¹, and Mabel Mphahlele-Makgwane¹

Abstract— Acid mine drainage (AMD) poses significant environmental challenges due to its low pH and high concentrations of dissolved metals. This study focuses on the synthesis and application of magnesium hydroxide ($Mg(OH)_2$) as a neutralizing agent for AMD. Magnesium hydroxide was synthesized by calcining magnesite at 800°C to produce magnesium oxide, followed by hydration. $Mg(OH)_2$ was then applied for AMD neutralization, raising the pH from 2.19 to 8.53, while reducing electrical conductivity (EC) from 451 to 390.5 $\mu S/cm$ and total dissolved solids (TDS) from 225.5 to 195.25 mg/L. The characterization of AMD was performed using Inductively Coupled Plasma Mass Spectrometry (ICP-MS) to determine the concentrations of heavy metals, while techniques such as X-ray Fluorescence (XRF), Fourier Transform Infrared Spectroscopy (FTIR), and Scanning Electron Microscopy (SEM) were used to analyse the solid samples. A comparative analysis with magnesite and magnesium oxide (MgO) revealed that synthesized magnesium hydroxide was the most effective in achieving pH, EC, and TDS values within SANS-241 water quality standards. These results underscore the potential of synthesized magnesium hydroxide for efficient AMD remediation.

Keywords— Acid Mine Drainage; Magnesium Hydroxide; Neutralization; Water Treatment.

I. INTRODUCTION

Water scarcity is one of the most pressing challenges in South Africa. With a growing population and increasing demands from agriculture, industry, and domestic sectors, the supply of clean water is becoming alarmingly limited [1]. Many communities still lack access to safe water sources, and this is compounded by the contamination of water bodies through various pollutants, one of the most serious being Acid Mine Drainage (AMD) [2]. AMD is a byproduct of mining operations and forms when sulfide minerals, especially pyrites, are exposed to air and water, leading to chemical reactions that generate sulfuric acid and dissolved heavy metals [1].

AMD is notorious for its severe environmental impact, often leading to contamination of both surface groundwater sources. The release of metals such as iron, manganese, and aluminum into water bodies disrupts ecosystems, reduces biodiversity, and poses significant risks to human health. Additionally, the low

pH levels of AMD (as acidic as 2-3) further degrade water quality, making it unfit for human consumption or agricultural use [2]. This issue has profound socio-economic implications, particularly in mining regions, where communities rely on these water sources for their livelihoods.

Efforts to remediate AMD have led to various treatment strategies, ranging from passive to active approaches. Techniques such as ion-exchange, adsorption, bio-sorption, and neutralization have been employed with varying degrees of success [3]. However, these methods often face challenges, including high operational costs, the production of secondary waste like sludge, and limited long-term effectiveness. The need for sustainable and cost-effective solutions has driven interest in alternative treatment methods.

Magnesium hydroxide ($Mg(OH)_2$) has emerged as a promising treatment option for AMD. It offers a unique advantage due to its strong alkaline nature, which helps neutralize the acidity of AMD. When introduced to acidic mine water, magnesium hydroxide reacts with sulfuric acid to form magnesium sulfate and water, raising the pH and facilitating the precipitation of metal hydroxides [4]. This process not only reduces metal contamination but also minimizes secondary pollution risks associated with other chemical treatments.

The use of magnesium hydroxide in AMD treatment also has practical benefits. It is relatively easy to apply, whether in the form of a slurry or through passive systems like permeable reactive barriers. Additionally, magnesium hydroxide exhibits a sustained buffering capacity, which allows it to provide long-term pH stabilization and metal precipitation [5]. Its ability to offer continuous water quality improvement makes it a viable option for large-scale remediation projects.

Despite its advantages, the application of magnesium hydroxide requires careful consideration of dosage and monitoring. Excess magnesium in treated water can lead to ecological imbalances or toxicity in aquatic life, necessitating a balance between effective treatment and environmental safety [6]. Nevertheless, its environmentally friendly profile and potential for large-scale use makes magnesium hydroxide a compelling candidate for addressing the AMD problem.

In South Africa, the severity of AMD and its far-reaching impacts cannot be overstated. AMD affects major water systems, including rivers that supply water to both rural and

Jacobeth Galane¹ is with the University of Limpopo, Department of Water and Sanitation Private Bag x1106, Sovenga, 0727, South Africa

Tholiso Ngulube¹, is with the University of Limpopo, Department of Water and Sanitation Private Bag x1106, Sovenga, 0727, South Africa

Mabel Mphahlele-Makgwane¹ is with the University of Limpopo, Department of Water and Sanitation Private Bag x1106, Sovenga, 0727, South Africa

urban populations. The economic implications are vast, as contaminated water impairs agricultural productivity, reduces property values, and increases the costs of water treatment. Addressing this issue is critical not only for protecting the environment but also for ensuring water security in regions affected by mining activities.

This research explores the efficacy of magnesium hydroxide synthesized from magnesite as a solution to neutralize AMD. By examining the interactions between magnesium hydroxide and AMD, the study aims to demonstrate the compound's potential to reduce acidity, precipitate harmful metals, and ultimately improve water quality. The findings could contribute to more sustainable remediation practices and provide a valuable framework for addressing AMD in South Africa and beyond.

II. MATERIALS AND METHODS

A. Sampling

AMD sample was collected from Khwezela Colliery open cast mine in Mpumalanga province, South Africa with GPS coordinates: (25.8891° S, 29.2320° E) and magnesite was purchased from Strathmore magnesite mine in Mpumalanga province, South Africa as well.

B. Preparation of Magnesite

Magnesite was obtained in its powdered form and used directly for the experiments. To ensure uniform particle size, the magnesite powder was passed through an 850 μm sieve. This step was critical to achieve consistency in particle size, which is necessary for maintaining uniformity throughout the experimental procedures. The sieved magnesite powder was then carefully stored in airtight plastic bottles to prevent contamination and moisture absorption, ensuring it remained in optimal condition for the subsequent calcination process.

C. Calcination And Hydration Studies

1) Calcination of Magnesite to Produce Magnesium Oxide

For calcination, 50 g of magnesite was calcined at 800°C for 60 minutes. After the calcination, the samples were allowed to cool to room temperature. The cooled samples were then hand-ground using a porcelain mortar and pestle to break down any large lumps. The ground samples were sieved through an 850 μm sieve to achieve a uniform particle size.

2) Hydration Procedure of Magnesium Oxide to Magnesium Hydroxide.

For hydration, 10 g of the calcined magnesite samples were weighed and stirred at a constant rate of 250 rpm in 100 mL of deionized water. The reaction was carried out using a hotplate and magnetic stirrer at temperatures ranging between 30°C and 80°C for 30 minutes.

3) Post-Hydration Processing.

At the end of each experiment, the slurry was vacuum filtered using a Büchner funnel connected to an Erlenmeyer flask with a rubber adapter to ensure a tight seal, and a tube connected to a vacuum pump was used to pull the liquid through the filter

paper. The solids remaining on the filter were washed twice with 50 mL of deionized water. The washed solids were dried in an oven at 105°C for one hour to prevent overheating. After drying, the solids were hand-ground with a porcelain mortar and pestle and then sieved through an 850 μm sieve for uniformity. To prevent additional oxidation and precipitation, the Mg (OH)₂ samples were stored in High-Density Polyethylene (HDPE) containers and maintained at a low temperature of 4°C until they were ready for neutralization in the laboratory, as recommended by [7].

D. Preparation of AMD samples.

The collected AMD samples were stored in closed HDPE bottles to prevent further oxidation and metal precipitation. These bottles were kept at 4°C until they were used for neutralization experiments. Before utilization, the AMD samples were filtered through a 0.4 μm perforated filter to remove any particulate matter.

E. Characterization Studies

1) Characterization of AMD

The metal content of AMD was characterized using ICP-MS instrument with the method of ME-011 for the determination of metals. A pH/ EC meter ((HACH HQ40D, Aqua-lytic, South Africa) was used to determine the readings of EC and pH of the AMD sample. TDS was calculated using the formula: $\text{TDS} = \text{EC} \times 0.5$

2) Characterization of the Neutralizing Agent

The neutralizing agents and AMD sludge were characterized using various analytical techniques. Scanning Electron Microscopy (SEM) was performed using a Sigma VP FE-SEM (USA), where samples were mounted on stubs with carbon tape and coated with gold to enhance conductivity. The SEM provided detailed surface images of the samples. X-ray Fluorescence (XRF) analysis was conducted using a Bruker XRF spectrometer to determine the elemental composition of the synthesized powdered samples. Samples were placed in specialized cups, sealed with plastic film, and analyzed three times for reproducibility. Fourier Transform Infrared (FTIR) spectrometry was performed with a Bruker Alpha-Platinum ATR in transmission mode to obtain infrared spectra of the powdered samples. The OPUS software was used to analyze the integrated intensity of the bands. Finally, Particle Size Distribution was determined using Laser Diffraction (LD), with samples diluted in deionized water for proper dispersion before analysis. The resulting data was processed and saved in CSV format for further evaluation.

F. AMD Neutralization Experiments

For the neutralization experiments, varying dosages of magnesium hydroxide (1 g, 2 g, 3 g, 4 g, 5 g, and 6 g) were added to separate 250 mL beakers containing 100 mL of AMD. Each mixture was stirred at 200 RPM using an overhead stirrer for 60 minutes. After allowing the samples to settle, the water was filtered using Whatman Grade 42 filter paper, and the filtrate was collected for analysis. Using the optimum dosage of

1g magnesium hydroxide, further neutralization experiments were conducted to vary contact times (10, 20, 30, 40, 90, and 120 minutes) under the same stirring conditions. After settling, the water was filtered, and the physicochemical properties, including pH, TDS, temperature, EC, and turbidity, were measured. The experiments were repeated twice to ensure reliable results.

G. Data analysis

For calculating removal efficiency of metal species equation (1) was used:

$$\% \text{ Removal} = \left(\frac{C_o - C_f}{C_o} \right) \times 100 \dots \dots \dots (1)$$

Where: C_o = Initial concentration, C_f = Equilibrium concentration.

C_o represents the initial concentration of metals before neutralization, while C_f denotes the ultimate concentration of the following neutralization.

III. RESULTS AND DISCUSSIONS

A. Characterization Results

1) SEM analysis

Fig.1 shows the SEM images providing insights into structural evolution throughout the synthesis and treatment process.

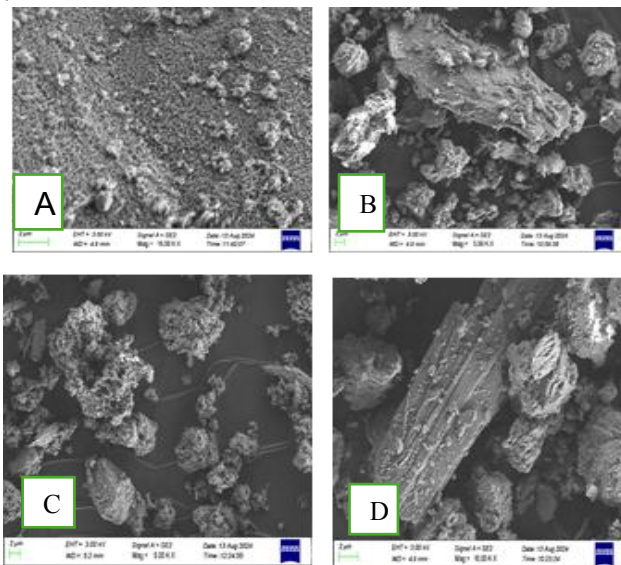


Fig.1 SEM images for A (Raw magnesite), B (Magnesium Oxide), C(Magnesium hydroxide) and D(AMD reacted sludge)

The SEM analysis reveals significant structural changes throughout the synthesis and treatment process. Raw magnesite shows a smooth, compact surface typical of its crystalline nature, supported by the XRF results indicating high MgO content. After calcination, the surface of magnesium oxide becomes porous and flaky, indicating increased surface area, which is linked to the decomposition of magnesite into MgO, as confirmed by XRF and FTIR. Magnesium hydroxide forms a plate-like structure with rough surfaces, enhancing its reactivity, supported by FTIR showing hydroxyl groups [7]. Finally, the AMD-reacted sludge exhibits an amorphous morphology, correlating with the precipitation of metal

hydroxides, as seen in XRF and FTIR results, confirming successful neutralization [8].

2) Particle size.

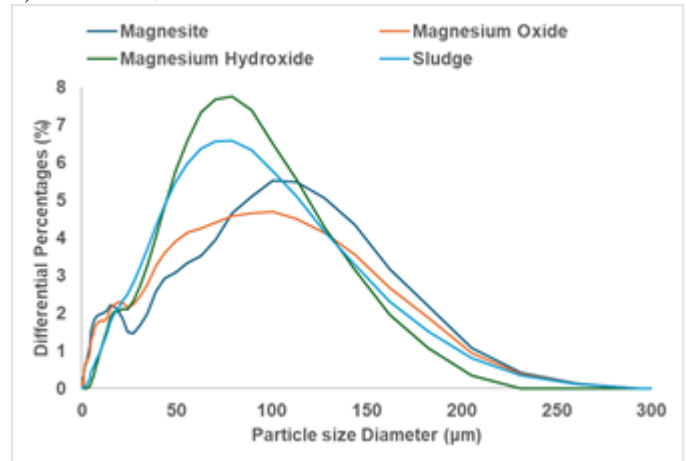


Fig. 2 Particle size distribution of different neutralising agents.

The particle size distribution of the neutralizing agents reflects the synthesis methods used, significantly influencing their reactivity. Magnesite, with a cumulative particle size of 133 µm at 90%, shows a sharp peak at 50 µm, indicating the formation of fine, uniform particles due to magnesium carbonate decomposition during calcination. Magnesium oxide, with a slightly lower cumulative size of 127 µm, follows a similar pattern, though broader due to variations in grinding or milling steps. Magnesium hydroxide, synthesized via hydration, exhibits a mean particle size of 50.07 µm and a broader distribution (116 µm at 90%), suggesting incomplete homogenization during synthesis, leading to varying particle sizes.

The AMD-reacted sludge demonstrates the widest distribution, peaking around 150 µm, due to its heterogeneous composition, including precipitated magnesium hydroxide and impurities from the treatment process. Finer particles, like those in magnesite, offer larger surface areas, enhancing neutralization efficiency, while the larger magnesium hydroxide particles may slow dissolution, affecting neutralization speed. The diverse particle sizes in the sludge indicate varying reactivity, potentially leading to prolonged neutralization effects over time. Particle size distribution is crucial for understanding the kinetics of neutralization, with smaller particles promoting faster reactions and larger ones possibly delaying complete neutralization [8].

3) XRF Analysis

Table I gives the elemental composition of the AMD.

TABLE I
ELEMENTAL COMPOSITIONS OF MAGNESITE, MAGNESIUM OXIDE,
MAGNESIUM HYDROXIDE AND AMD REACTED SLUDGE.

	Magnesite	MgO	Mg (OH) ₂	AMD reacted with Mg (OH) ₂ (Sludge)
Element Names	%	%	%	%
MgO	32.217	68.838	48.215	38.022
SiO ₂	8.022	9.699	8.816	6.152
CaO	1.345	1.775	1.697	3.501
Fe ₂ O ₃	1.307	1.442	1.273	4.842
Sn	0.039	0.018	0.020	0.016

The elemental composition of the neutralizing agents—magnesite, magnesium oxide, magnesium hydroxide, and the resulting sludge after treating acid mine drainage with magnesium hydroxide are presented in Table I. Magnesium oxide exhibits a notably higher magnesium content compared to both magnesite and magnesium hydroxide. The decrease in magnesium oxide in the sludge suggests active participation of magnesium in the neutralization process, forming precipitates such as magnesium sulfate. Silica content remains relatively stable across samples, with only a slight decrease in the sludge, indicating minimal involvement in chemical reactions during AMD treatment. The highest calcium oxide content is observed in the sludge, reflecting its role in precipitating as calcium sulfate (gypsum) during treatment.

This is further supported by ICP-MS results showing a significant reduction in calcium concentration after treatment. The Fe₂O₃ content in the sludge shows a substantial increase compared to lower values in the neutralizing agents, indicating the precipitation of iron as hydroxides or oxides when the pH is raised during treatment [8]. Lastly, tin is present in trace amounts across all samples, exhibiting minimal variation, suggesting it is not significantly affected by the neutralization process.

4) FTIR Analysis

FTIR spectrum of Magnesite, MgO, Mg (OH)₂ and a sludge of AMD reacted with Mg (OH)₂ are represented in fig. 3.

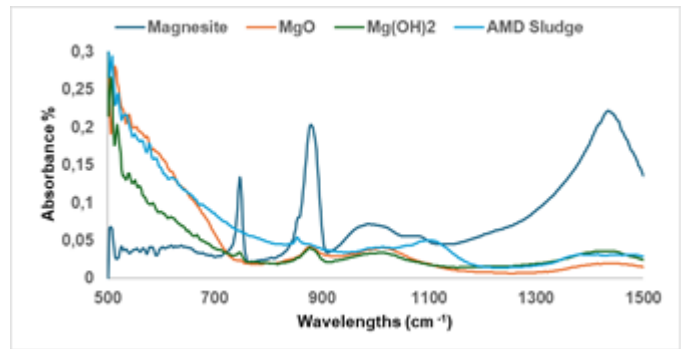


Fig. 3 FTIR scatter graph showing the spectrum of magnesite, MgO, Mg (OH)₂ and reared AMD sludge.

The FTIR analysis of magnesite, magnesium oxide (MgO), magnesium hydroxide (Mg (OH)₂), and AMD sludge reacted with Mg (OH)₂ reveals significant insights into their chemical structures and transformations. Magnesite exhibits characteristic carbonate stretching vibrations around 850 cm⁻¹ and 1450 cm⁻¹, confirming its composition as MgCO₃, with a doublet at 1450 cm⁻¹ indicating a mixture of magnesite and calcite. In MgO, the absence of carbonate peaks, along with a strong periclar stretch near 950 cm⁻¹, confirms the successful conversion of MgCO₃ to MgO through calcination.

Magnesium hydroxide displays a broad peak around 3700 cm⁻¹, indicating the presence of hydroxyl groups, alongside residual carbonate stretches around 850-950 cm⁻¹, suggesting some remaining carbonates. The AMD sludge reacted with Mg (OH)₂ also shows a broad hydroxyl peak at 3700 cm⁻¹, confirming the presence of OH groups from magnesium hydroxide. Additionally, peaks around 1100 cm⁻¹ and 1400 cm⁻¹ indicate the precipitation of metal species such as Al₂O₃ and Fe₂O₃, along with carbonates during AMD treatment [9]. Overall, the FTIR analysis highlights the structural transformations and successful neutralization of acidic mine drainage through synthesized magnesium hydroxide.

B. Physicochemical properties of AMD.

Table II shows the physicochemical properties of AMD before and after neutralization.

TABLE II
PHYSICOCHEMICAL PROPERTIES OF AMD BEFORE AND AFTER
NEUTRALIZATION.

Physicochemical properties	Before neutralization	After neutralization
pH	2.19	8.53
EC (µs/cm)	451	390.5
TDS (mg/L)	222.5	195.25

Before neutralization, the AMD had a pH of 2.19, confirming its highly acidic nature, with an electrical conductivity (EC) of 451 µs/cm and total dissolved solids (TDS) of 222.5 mg/L, indicating significant contamination by dissolved metals and sulfates. These conditions, typical of AMD, pose serious risks to aquatic life and contribute to the leaching of metals such as

iron and aluminum into the water [1], [10]. After neutralization with magnesium hydroxide, the pH increased to 8.53, demonstrating successful neutralization, while the EC decreased to 390.5 $\mu\text{s}/\text{cm}$, and TDS dropped to 195.25 mg/L. This reduction in ionic content reflects the precipitation of metal hydroxides, effectively lowering the concentration of dissolved metals and improving water quality [2], [11]. These results suggest that magnesium hydroxide effectively neutralizes AMD, reducing its environmental impact [12].

C. ICP-MS analysis

Table III gives the elemental composition of AMD.

TABLE III
ICP-MS RESULTS SHOWING THE ELEMENTAL COMPOSITIONS OF AMD BEFORE AND AFTER TREATMENT.

Element composition	Before neutralization (mg/L)	After neutralization (mg/L)
Potassium as K	15.75	2.05
Copper as Cu	0.001	0.001
Sodium as Na	65.50	8.36
Magnesium as Mg	512.24	69.84
Iron as Fe	0.003	0.001
Calcium as Ca	510.05	69.84
Sulphate as SO ₄	1881.68	310.25

The ICP-MS analysis demonstrates the efficiency of magnesium hydroxide in reducing metal concentrations in AMD. The removal percentages were significant, with magnesium showing a 93.26% reduction, potassium 86.30%, and iron 66.67% calculated using equation 1. The high initial concentration of magnesium is due to its abundance in the AMD, which is expected from the dissolution of minerals in acidic conditions. Its large reduction after treatment highlights the neutralizing effect of magnesium hydroxide, which likely precipitated magnesium ions as hydroxides. The sulphate levels in AMD were initially high, after treatment with the synthesized magnesium hydroxide, they were reduced significantly. Potassium's significant reduction can be attributed to its solubility in water, making it more responsive to the treatment process. Iron, though reduced by 66.67%, exhibited a lower removal efficiency compared to magnesium. This is likely due to the formation of iron hydroxides and oxides, which are less soluble at higher pH levels but may require additional treatments for complete removal.

D. Neutralization Study

Fig. 4 represents the variation of pH at different time intervals during neutralization experiments.

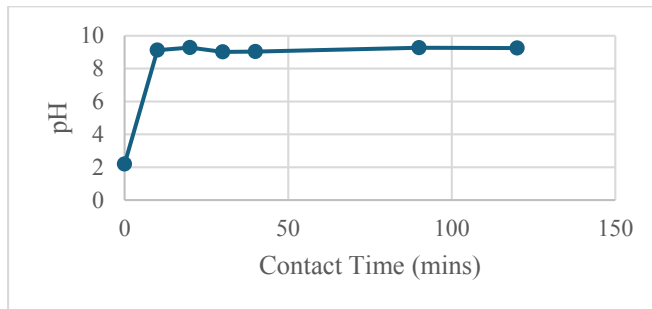


Fig.4 Variation of pH on neutralization of AMD using Mg(OH)₂ at different time.

Fig.4 shows the variation of pH during the neutralization of AMD using magnesium hydroxide over 120 minutes. Initially, the AMD has a highly acidic pH of 2.19, but upon the addition of magnesium hydroxide, the pH rapidly rises to 9.12 within the first 10 minutes, indicating fast neutralization. The pH peaks at 9.28 at 20 minutes, followed by a slight dip to 9.02 between 20 and 40 minutes, likely due to buffering reactions. The pH then recovers, reaching 9.27 by 90 minutes and stabilizing around 9.25 by 120 minutes, signifying that equilibrium has been achieved. This demonstrates magnesium hydroxide's effectiveness in quickly neutralizing AMD to alkaline levels.

Fig. 5 represents the variation of pH at different magnesium hydroxide dosages during neutralization experiments.

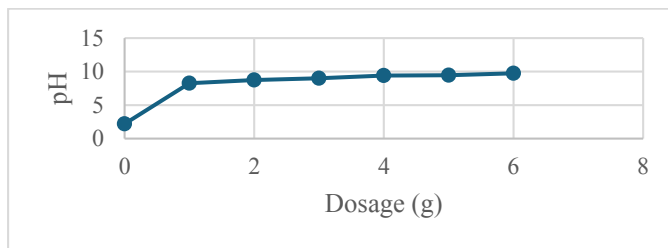


Fig. 5 Variation of pH on the neutralization of AMD using various dosages at 60 minutes.

Fig. 5 shows that as the dosage of magnesium hydroxide increases, the pH of the mine water steadily rises from 8.3 to 9.8, indicating that magnesium hydroxide effectively neutralizes acidity. Each increase in dosage results in a higher pH, demonstrating a strong correlation between the amount of magnesium hydroxide added and the increased alkalinity of the water. This suggests that higher dosages lead to more effective treatment of acidic mine water.

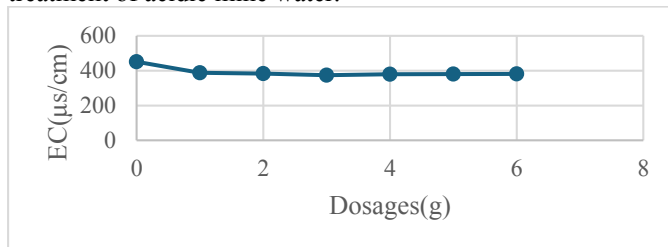


Fig. 6 The response of EC on the neutralisation of AMD at different time intervals using 1g of Mg(OH)₂ dosage.

Fig.6 shows different dosages influencing electrical conductivity (EC) of mine water. EC is an indicator of water quality [13]. The graph initially showed a rapid decrease in EC when 1g dosage was introduced showing the effectiveness of magnesium hydroxide and the subsequent increase in EC could result from the dissolution of metal ions as the pH rises, releasing new ions into the solution and raising the conductivity.

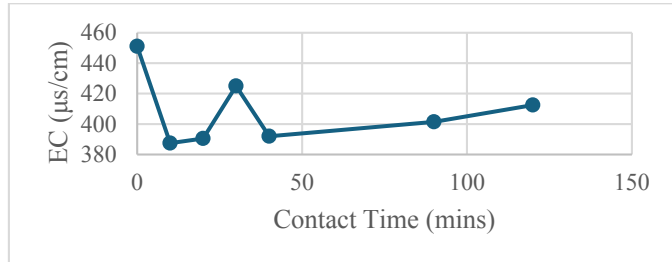


Fig 8 The response of EC on the neutralisation of AMD on different Mg(OH)₂ dosages.

Initially, at 10 minutes, the EC increases as metal ions or salts dissolve due to the rising pH. This is followed by a rapid rise in EC at 20 minutes, likely due to a significant reaction or the release of additional ions. At 30 minutes, there is a noticeable decrease in EC, which could be attributed to the precipitation of metal hydroxides as the pH stabilizes, reducing the concentration of dissolved ions. The subsequent increases in EC from 40 to 120 minutes suggest ongoing ion exchange or further dissolution of magnesium ions, reflecting the complex and dynamic nature of the treatment process.

E. Comparison of Physicochemical Characteristics Using Different Neutralizing Agents After Neutralization.

The comparison of neutralizing agents for treating AMD showed that synthesized magnesium hydroxide was the most effective in achieving a pH within the SANS 241 acceptable range for drinking water (6.5-8.5). While magnesite resulted in a highly acidic pH of 2.30 and magnesium oxide (MgO) raised the pH to an excessive 9.21, synthesized magnesium hydroxide neutralized the AMD to a pH of 8.53, which is within permissible limits. In terms of EC and TDS, all three agents produced similar results, with EC values around 386-391 µS/cm and TDS between 189-195 mg/L, well within the acceptable limits. Overall, synthesized magnesium hydroxide proved to be the most effective agent, achieving optimal pH without significantly increasing ion concentrations or TDS levels.

ACKNOWLEDGEMENT

The authors would like to acknowledge the Department of Water and Sanitation, University of Limpopo for providing resources to make this research possible.

REFERENCES

- [1] P.K. Sahoo, S. Tripathy, M.K. Panigrahi, and S.M. Equeenuddin, "Anthropogenic contamination and risk assessment of heavy metals in stream sediments influenced by acid mine drainage from a northeast coalfield, India," *Bulletin of Engineering Geology and the Environment*, vol. 76, pp. 537-552, 2017. <https://doi.org/10.1007/s10064-016-0975-2>
- [2] J.O. Ighalo, S.B. Kurniawan, K.O. Iwuozor, C.O. Aniagor, O.J. Ajala, S.N. Oba, F.U. Iwuchukwu, S. Ahmadi, and C.A. Igwegbe, "A review of treatment technologies for the mitigation of the toxic environmental effects of acid mine drainage (AMD)," *Process Safety and Environmental Protection*, vol. 157, pp. 37-58, 2022. <https://doi.org/10.1016/j.psep.2021.11.008>
- [3] G. Chen, Y. Ye, N. Yao, N. Hu, J. Zhang, and Y. Huang, "A critical review of prevention, treatment, reuse, and resource recovery from acid mine drainage," *Journal of Cleaner Production*, vol. 329, p. 129666, 2021. <https://doi.org/10.1016/j.jclepro.2021.129666>
- [4] L. Szymoniak, D. Claveau-Mallet, M. Haddad, and B. Barbeau, "Application of magnesium oxide media for remineralization and removal of divalent metals in drinking water treatment: A review," *Water*, vol. 14, no. 4, p. 633, 2022. <https://doi.org/10.3390/w14040633>
- [5] RoyChowdhury, D. Sarkar, and R. Datta, "Remediation of acid mine drainage-impacted water," *Current Pollution Reports*, vol. 1, pp. 131-141, 2015. <https://doi.org/10.1007/s40726-015-0011-3>
- [6] P. Kannan, F. Banat, S.W. Hasan, and M.A. Haija, "Neutralization of Bayer bauxite residue (red mud) by various brines: A review of chemistry and engineering processes," *Hydrometallurgy*, vol. 206, p. 105758, 2021. <https://doi.org/10.1016/j.jece.2018.02.005>
- [7] V. Masindi, J.G. Ndiritu, and J.P. Maree, "Fractional and step-wise recovery of chemical species from acid mine drainage using calcined cryptocrystalline magnesite nano-sheets: An experimental and geochemical modelling approach," *Journal of Environmental Chemical Engineering*, vol. 6, no. 2, pp. 1634-1650, 2020. <https://doi.org/10.1016/j.jece.2018.02.005>
- [8] Y. Ma, X. Liu, X. Zhao, and H. Wang, "Synthesis and Characterization of Magnesium Hydroxide Nanoparticles via Hydration Process for Enhanced Environmental Applications," *Journal of Materials Chemistry*, vol. 28, no. 5, pp. 1357-1364, 2020.
- [9] G. Kaur, S. J. Couperthwaite, B. W. Hatton-Jones, and G. J. Millar, "Alternative Neutralization Materials for Acid Mine Drainage Treatment," *Journal of Water Process Engineering*, vol. 22, pp. 46-58, 2018. <https://doi.org/10.1016/j.jwpe.2018.01.004>
- [10] Luo, J. Routh, M. Dario, S. Sarkar, L. Wei, D. Luo, and Y. Liu, "Distribution and Mobilization of Heavy Metals at an Acid Mine Drainage Affected Region in South China, a Post-Remediation Study," *Science of the Total Environment*, vol. 724, p. 138122, 2020. <https://doi.org/10.1016/j.scitotenv.2020.138122>
- [11] M. J. Alegbe, B. A. Moronkola, A. O. Elesho, O. S. Ayanda, and L. F. Petrik, "Physicochemical Characterization of Tin Oxide Synthesized from Acid Mine Drainage Using Tin II Chloride," *American Journal of Chemistry*, vol. 12, no. 1, pp. 10-17, 2022.
- [12] V. Akinwekomi, J. Maree, V. Masindi, C. Zvinowanda, M. Osman, S. Foteinis, L. Mpenyana-Monyatsi, and E. Chatzisyseon, "Beneficiation of acid mine drainage (AMD): A viable option for the synthesis of goethite, hematite, magnetite, and gypsum—Gearing towards a circular economy concept," *Minerals Engineering*, vol. 148, pp. 106-204, 2020. <https://doi.org/10.1016/j.mineng.2020.106204>
- [13] S. Fourie and R. Steenkamp, "The Pit Bull and the Obstacle Course—Journey of a Dragline," *Civil Engineering= Siviele Ingenieurswese*, vol. 2020, no. 3, pp. 12-18, 2020.
- [14] G. W. Gee and D. Or, "2.4 Particle-Size Analysis," in *Methods of Soil Analysis: Part 4 Physical Methods*, vol. 5, pp. 255-293, 2020. <https://doi.org/10.2136/sssabookser5.4.c12>